Electronic and phonon instabilities in face-centered-cubic alkali metals under pressure studied using *ab initio* calculations

Yu Xie,[1] John S. Tse,[2] Tian Cui,[1] Artem R. Oganov,[3] Zhi He,[1] Yanming Ma,[1,3,*] and Guangtian Zou[1]
[1]*National Lab of Superhard Materials, Jilin University, Changchun 130012, China*
[2]*Department of Physics and Engineering Physics, University of Saskatchewan, Saskatoon S7N 5E2, Canada*
[3]*Laboratory of Crystallography, Department of Materials, ETH Zurich, HCI G 515, Wolfgang-Pauli-Strasse 10, CH-8093 Zurich, Switzerland*

(Received 18 July 2006; revised manuscript received 28 November 2006; published 2 February 2007)

The evolution of Fermi surfaces and lattice dynamics for alkali metals in the fcc structure with pressure have been studied using *ab initio* calculations within the density functional theory. Fermi surface nesting features along the Γ-K symmetry direction in the Brillouin zone have been identified for Li, K, Rb, and Cs, while it is absent for Na. Moreover, a transverse acoustic phonon softening along the Γ-K with pressure is predicted for Li, Na, K, Rb, and Cs. This observation suggests a common phonon softening behavior in fcc alkali metals at high pressure. Analysis of the theoretical results suggests that the consideration of both phonon and electronic instabilities is crucial to the understanding of pressure-induced phase transitions in the fcc alkali metals.

DOI: 10.1103/PhysRevB.75.064102 PACS number(s): 62.50.+p, 64.70.Kb, 63.20.Dj, 71.18.+y

Alkali metals are usually considered as simple metals because of the simple electronic structure with just one conduction electron outside the closed-shell configurations. The nearly free electron model is known to be a good approximation to describe their electronic properties due to the weak interaction between valence electrons and ionic core under ambient conditions.[1] However, under high pressure, the nearly free electron description of alkali metals fails as evidenced by the complex sequence of phase transitions.[2] Alkali metals having the bcc structure at low pressure transform to an fcc modification for Li at 7.5 GPa,[3] Na at 65 GPa,[4] K at 11.5 GPa,[5] Rb at 7 GPa,[6] and Cs at 2.3 GPa,[7] respectively. The bcc→fcc transition in alkali metals has been attributed to $s \rightarrow d$ electrons transfer for K, Rb, and Cs, and $s \rightarrow p$ electrons transfer for Li.[8] At higher pressure all alkali metals with fcc structure transform into more complex structures. Specifically, Li at 39 GPa,[9] Na at 103 GPa,[4] K at 19 GPa,[10] Rb at 13 GPa,[11] and Cs at 4.2 GPa[12] transform to R-3m,[9] I-43d,[13] host-gust composite structure,[10] $C222_1$,[11] and $C222_1$ (Ref. 12) structures, respectively.

Very recently, several theoretical studies[14–18] have contributed to the understanding of the enhanced superconducting transition temperature (T_c) with increasing pressure for fcc Li. It is now accepted that the combination of a Fermi surface nesting (FSN) with a transverse acoustic (TA) phonon softening along the Γ→K symmetry direction is responsible for the relatively high T_c for fcc Li[14,15] at high pressure. Moreover, the possible superconductivities in Na and K have been predicted theoretically by Sanna *et al.*[16] for K and Shi and Papaconstantopoulos[18,19] for K and Rb, respectively. Much experimental effort is needed to clarify the validity of these theoretical predictions. However, the physical mechanism driving the phase transition from fcc to the complex structures in alkali metals is less studied. Electronic (FSN)[20] and dynamic instabilities[21] are often responsible for phase transitions under pressure. In a previous study on fcc Cs,[22] a softening of the TA phonons near the zone center was identified and attributed to the transition mechanism for the fcc Fm-3m to $C222_1$ phase transition. Recently, Rodriguez-Prieto and Bergara[23] suggested that an FSN at 30 GPa could be the origin of the complex phase transitions for fcc lithium. In this work, we investigate systemically the evolution of Fermi surface and lattice dynamics with pressure in alkali metals with the fcc structure in order to probe the nature of the phase transition to high-pressure complex structures. We found a TA phonon softening along the Γ-K symmetry direction with pressure in all fcc alkali metals. Besides Li, FSN along Γ-K in the Brillouin zone (BZ) is also identified for K, Rb, and Cs, while it is absent for Na. It is shown that both the TA phonon softening and FSN are closely related to the phase transitions.

Lattice dynamics for alkali metals at high pressure are investigated using the pseudopotential plane-wave (PP) density-functional linear-response method.[24] The local density approximation (LDA) exchange-correlation functional is employed.[25] The Troullier-Martins (TM)[26] norm-conserving scheme is used to generate a tight pseudopotential for Li, Na, K, Rb, and Cs with the electronic configurations of $2s^1$ and $3s^1$ (with nonlinear core correction), $3p^6 4s^1$, $4p^6 5s^1$, and $5p^6 6s^1$, respectively. Convergence tests gave a kinetic energy cutoff, E_{cutoff}, as 80 Ry and a 16×16×16 Monkhorst-Pack (MP) grid for the electronic BZ integration. A 16×16×16 MP **k** mesh was found to yield phonon frequencies converged to within 0.05 THz. Fermi surface calculations for alkali metals are performed using the full-potential (FP) linearized augmented plane wave method, through WIEN2K,[27] within the density functional theory (DFT).[28] The electron exchange-correlation energy is described in the generalized gradient approximation (GGA).[29] The cutoff of the plane-wave expansion was given by $RK_{\max}=9$. Convergence tests gave the use of 10 000 **k** points for the self-consistent calculation in the BZ. A large set of 32 768 **k** points was chosen for the calculation of the Fermi surfaces.

The theoretical equilibrium lattice constants and equation of states (EOS) of the fcc structure for the alkali metals studied here were determined by fitting the total energies as a function of volume to the 3rd-order Birch-Murnahan EOS.[30] The calculated equilibrium lattice parameters (a_0), bulk

TABLE I. Calculated equilibrium lattice parameter (a_0), bulk modulus (B_0), and the pressure derivative of bulk modulus (B_0') for fcc Li, Na, K, Rb, and Cs, respectively. Previous theoretical calculations (Refs. 4, 22, 31, and 32) and the experimental results (Refs. 3, 4, and 33–35) through the fitting of equation of states are also shown for comparison.

Alkali metals		a_0 (a.u.)	B_0 (GPa)	B_0'
	FP	8.17	13.61	3.55
Li	PP	8.16	15.23	2.66
	Ref. 31	8.08	13.76	3.28
	Expt.	8.29[a]	13.10[b]	2.80[b]
	FP	10.01	7.43	3.86
Na	PP	9.85	10.79	2.64
	Ref. 4	10.06	6.85	3.92
	Expt.	10.21[c]	6.43[c]	3.84[c]
	FP	12.54	3.82	3.7
K	PP	12.33	4.52	2.8
	Ref. 31	12.15	4.4	4.1
	Expt.	12.43[d]	4.25[d]	3.63[d]
	FP	13.54	3.23	3.38
Rb	PP	13.27	3.54	2.37
	Ref. 32	12.82	4.90	
	Expt.	12.98[d]	5.83[d]	2.08[d]
	FP	14.58	2.23	3.23
Cs	PP	14.33	2.99	3.46
	Ref. 22	13.87	2.20	
	Expt.	14.71[e]		

[a]Reference 33
[b]Reference 3.
[c]Reference 4.
[d]Reference 34.
[e]Reference 35.

modulus (B_0), and the pressure derivative (B_0') within PP and FP methods together with other theoretical results and the experimental data are listed in Table I. The theoretical lattice constants are in good agreement with experimental data within 1.4%, 3.5%, 0.8%, 4.3%, and 0.9% for Li, Na, K, Rb, and Cs, respectively. The calculated EOS of alkali metals in fcc structure within PP and FP methods are compared with the experimental data[3,4,33–35] as shown in Fig. 1. The agreement between theory and experiment is excellent for Li and Na. Therefore, the current PP and FP calculations at the same volume will produce almost identical pressure for Li and Na. Note that the PP EOS for K, and the FP EOSs for Rb and Cs agree also well with the experimental measurements. However, there are some noticeable discrepancies between theory and experiment for FP calculation in K, and PP calculations in Rb and Cs. Specifically, the FP EOS in K overestimates an experimental pressure of ~2 GPa, while the PP results in Rb and Cs underestimate the experimental pressures of ~2 GPa and ~0.5 GPa, respectively. Therefore, all the calculated pressures below within FP theory in K and PP theory in Rb and Cs will be corrected with pressures of −2, 2, and 0.5 GPa, respectively, to guarantee the current FP and PP calculations producing exactly the experimental pressures.

The evolution of two-dimensional (2D) sections of the Fermi Surface (FS) with pressure is explored on the reciprocal lattice planes (001) and (110) in the first BZ. These choices are guided by the observed significant changes in the band structures near the Fermi level along Γ-K-W-X, Γ-X, and Γ-L directions for Li, K, Rb, and Cs[16,32,36] at high pressure. Figure 2 summarizes the change of the FS with pressure for Li. At zero pressure, the perfect circular feature in the 2D FS in both the (001) and (110) planes indicates a nearly free electron character. At increased pressure, while there is no noticeable change in the FS in the (100) plane (bottom row of Fig. 2), the circular feature in the (110) plane which includes the Γ, L, and K points (top row of Fig. 2) starts to distort at 10 GPa and finally disappears. This observation indicates that a free electron description of Li is no longer valid at very high pressure. It is significant that at 30 GPa, the FS develops into two parallel planes with a nesting vector of 0.71 (110) along the Γ-K direction. A FSN suggests the possibility of a structural instability which might be related to the observed structural phase transition from fcc to R-3m. The predicted FSN of Li at 30 GPa is in excellent agreement with the results reported in Refs. 14 and 22.

The calculated evolution of the 2D FS with pressure for Na is shown in Fig. 3. With increasing pressure, the FS shows negligible change in both reciprocal lattice planes. Incidentally, the nearly free electron model seems still to be valid for Na even up to 105 GPa.

Figure 4 displays the change of the 2D FS with pressure for fcc K. It is found that the spherical FS is destroyed with increasing involvement of localized 3d orbital with increasing pressure. In the (110) plane the 2D FS shows a FSN feature at 8 GPa, indicating a possible structural instability for the fcc structure. At 11 GPa, the parallel FS feature starts to vanish. The electronic instability due to FSN might be related to the reversible phase transition of fcc→bcc under uncompressing. Concerning the contrasting behavior observed in Li, we have carefully re-examined the FS and phonon calculations. We observed no hint of both dynamical and electronic stability at low pressure for Li. The reverse fcc →bcc transition in Li therefore is not driven by phonon and electronic instability but rather by the energetic. It is significant that at 18 GPa, a second FSN feature for K appeared in the (100) plane with parallel FS along the Γ-K direction with a nesting vector of 0.58 (110) in Fig. 4. On the other hand, the FSN feature in the (110) plane has completely disappeared. The appearance of the FSN feature at 18 GPa coincides with the observed structural phase transition pressure of 19 GPa from fcc to the host-gust composite structure for K.[10] In addition, we also explore the 2D FS parallel to the ΓXK plane. The results are plotted in Fig. 5. It is very interesting to note that at ~0.6ΓX [Fig. 5(e)], possible nesting of the FS parallel to the Γ→X direction is predicted. The more complex FS of K reveals that there are more possibilities of electronic instability other than just in the [110] direction, as observed in Li.[23]

Figures 6 and 7 show the development of the 2D FS with pressure for Rb and Cs, respectively. The evolution of the FS topology for Rb and Cs is very similar to that predicted for

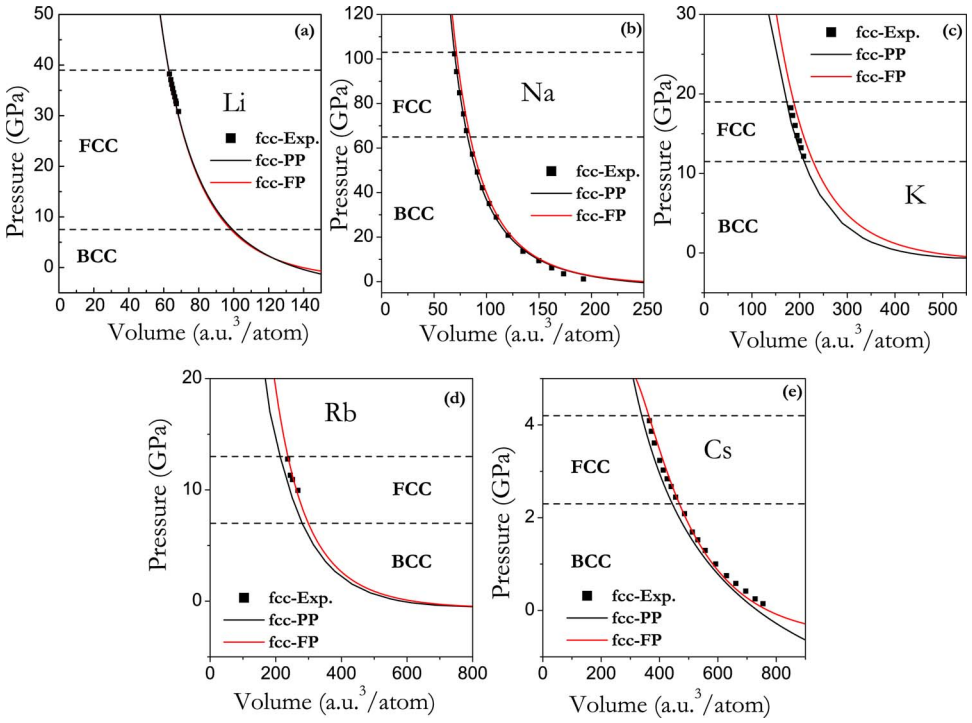

FIG. 1. (Color online) Comparison of the calculated equation of states (solid line) for the fcc Li (a), Na (b), K (c), Rb (d), and Cs (e) with the experimental data (solid square symbols). The red lines are the results from FP method and the black lines are the results from PP method.

K. It is important that in the (110) plane, FSN characters appeared at 3 GPa and 0 GPa, but disappeared at 6 GPa and 1 GPa for Rb and Cs, respectively. The predicted FSN in (110) plane for Rb and Cs might also be related to the reversible phase transition of fcc→bcc when the pressure was released. New FSN features in the (100) plane for Rb and Cs are predicted at 13.2 GPa and 4 GPa, respectively. The estimated nesting vectors are all 0.58 (110) for Rb and Cs. It should be pointed out that the predicted pressures on the appearance of the FS instabilities are very close to the observed phase transition pressures of 13 GPa and 4.2 GPa for Rb and Cs from fcc to the more complex $C222_1$ structures. Note also that the extended 2D FS (not shown) parallel to the Γ*XK* plane for Rb and Cs at 13.2 GPa and 4 GPa, respectively, are almost identical to that of K plotted in Fig. 5.

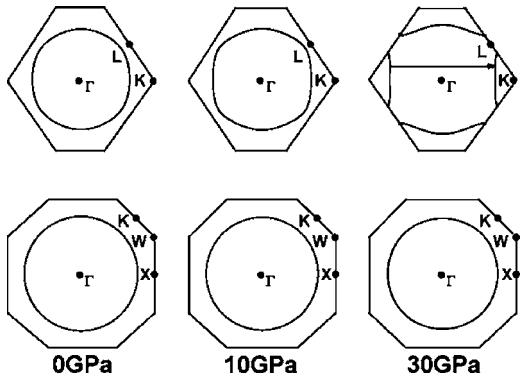

FIG. 2. Fermi surface cross sections of fcc Li at 0, 10, and 30 GPa along (110) (upper panel) and (100) (lower panel) planes. Although the Fermi surface along the (100) plane shows an almost perfect circle, it becomes highly distorted in the (110) plane with a clearly nesting along the Γ-K direction at 30 GPa. The arrows represent nesting vectors.

Figure 8 shows the calculated angular momentum decomposed DOS divided by total DOS at Fermi level for fcc Li, Na, K, Rb, and Cs with volume. From the analysis of the partial DOS in Fig. 8(b), it is shown that at zero pressure, the 3*p* orbital for Na is occupied at about 50% in fcc structure. With increasing pressure it increases slowly up to the border line of fcc/post-fcc. When the pressure is increased beyond 103 GPa (V/V_0=0.29), the 3*d* orbital starts to become significant. This observation is in good agreement with the report of Neaton and Ashcroft.[37] To obtain further information on the electron topology, variation of the 3D FS with pressure is also studied. It was also found that the almost spheri-

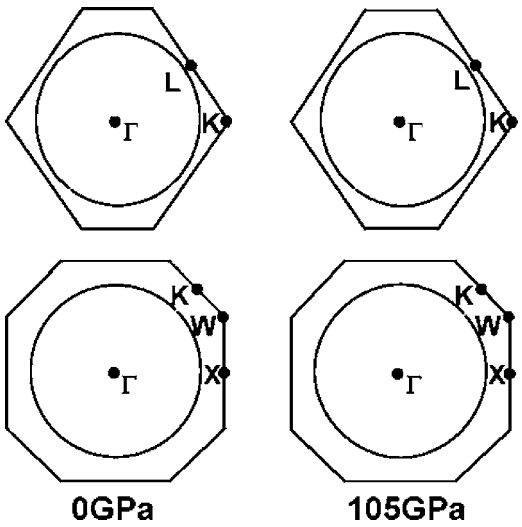

FIG. 3. Fermi surface cross sections of fcc Na at 0 and 105 GPa along (110) (upper panel) and (100) (lower panel) planes. With increasing pressure, there are no noticeable changes in FS for both planes.

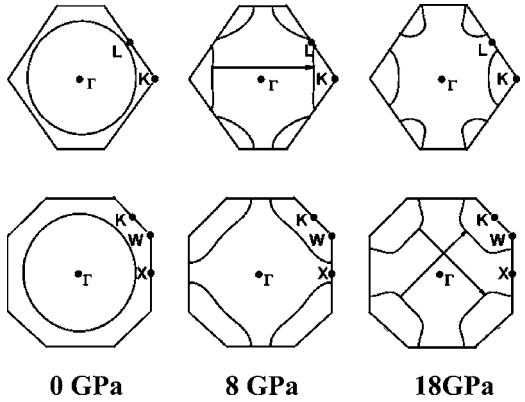

FIG. 4. Fermi surface cross sections of fcc K at 0, 8, and 18 GPa along the (110) (upper panel) and (100) (lower panel) planes. The arrows represent nesting vectors.

cal nature of the FS does not change at 105 GPa, even up to 242 GPa. From Fig. 8(a), one observes that in Li, the *p*-DOS contribution in the fcc structure is already very significant (80%) even at low pressure (large volume) and increase steadily at the expense of decreasing *s* character. The increased *p* contribution eventually led to the formation of a hole in the FS near the L point. In contrast, in Na, although the *s* contribution at low pressure in the stability region of the bcc phase decreases, the *p* contribution remains largely the same at 55%. More importantly, the *p* contribution in the fcc phase (from V/V_0=0.346–0.29) is almost constant at 57% to the total DOS, while the *d* contribution increases slightly but remains small. For this reason, there is only minor distortion in the FS near the observed phase transition at 105 GPa. This might be the reason for the persistence of the spherical FS in Na at high pressure up to 105 GPa. It is noteworthy that the significant differences in FS between Na and Li under high pressure might also be attributed to differences in the valence-core interactions.[37] For the heavier K,

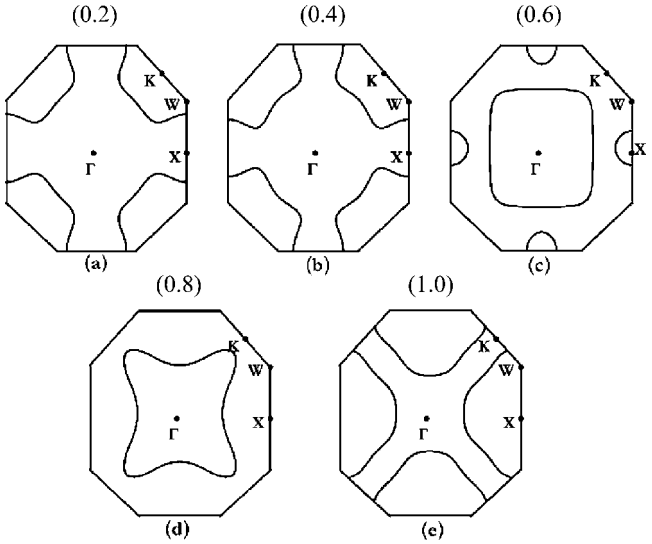

FIG. 5. Fermi surface cross sections (solid lines) of fcc-K at 18 GPa along planes parallel to the Γ*KX* plane at 0.2 (a), 0.4 (b), 0.6 (c), 0.8 (d), and 1.0 (c) times the Γ*X* distance.

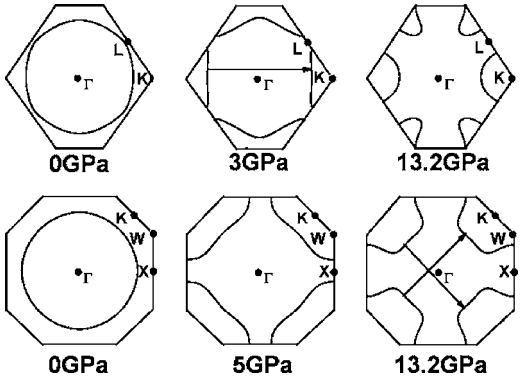

FIG. 6. Fermi surface cross sections of fcc Rb at 0, 3, and 13.2 GPa along (110) plane (upper panel) and at 0, 5, and 13.2 GPa along (100) plane (lower panel). The arrows represent nesting vectors.

Rb, and Cs in Figs. 8(c)–8(e), we indeed observed that at the pressure close to the FSN, the *d*-DOS increases significantly. It should also be pointed out that the current calculations for partial DOS in K and Rb are in excellent agreement with the previous calculation by Shi and Papaconstantopoulos.[19]

Preliminary phonon dispersion calculations were performed with the force constant interpolation method using the linear response approach. Phonon softening is identified for all the alkali metals along the Γ-K direction at high pressures. The calculated results agree well with those reported in Refs. 14 and 15 for Li, in Ref. 16 for K, and in Ref. 22 for Cs. To obtain very accurate phonon dispersion, phonon frequencies for individual *q* points along the Γ-K direction were calculated explicitly to eliminate possible interpolation errors in the force constant method. Figure 9 shows the directly calculated phonon results with pressure for Li, Na, K, Rb, and Cs, respectively. It is quite clear that with increasing pressure all the five alkali metals with the fcc structure show TA phonon softening that may induce structural instability. Imaginary phonon modes for Li, Na, K, Rb, and Cs start to appear at 33 GPa, 103 GPa, 28 GPa, 17 GPa, and 4 GPa, respectively. The predicted pressures correlate nicely with the experimentally measured structural transition pressures of 39 GPa, 103 GPa, 19 GPa, 13 GPa, and 4.2 GPa in fcc Li, Na, K, Rb, and Cs, respectively. For a summary, Table II lists

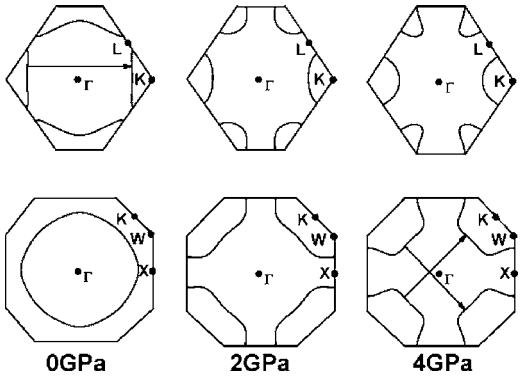

FIG. 7. Fermi surface cross sections of fcc Cs at 0, 2, and 4 GPa along (110) (upper panel) and (100) (lower panel) planes. The arrows represent nesting vectors.

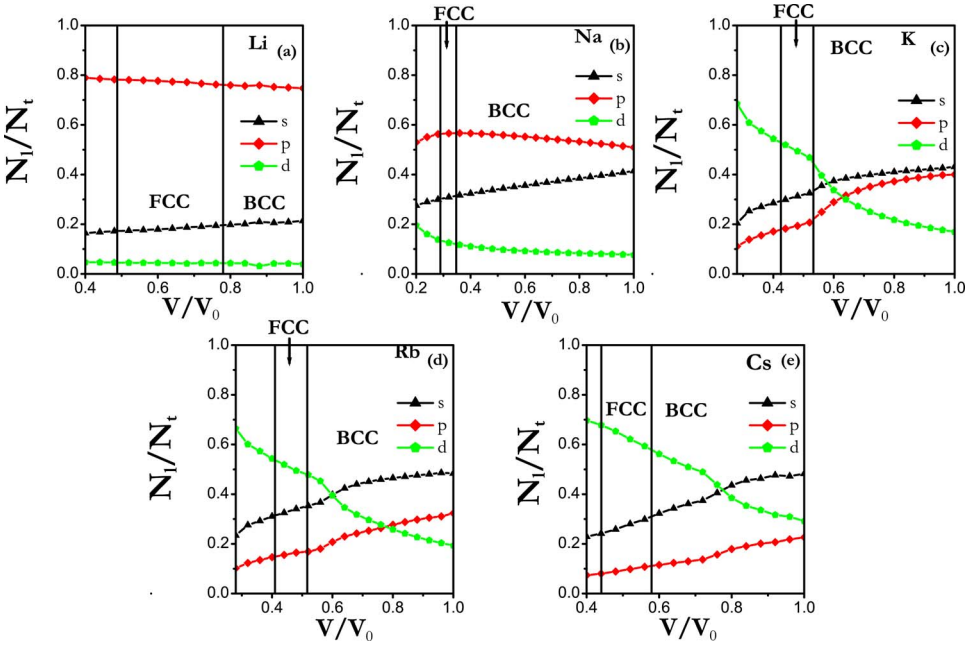

FIG. 8. (Color online) The calculated angular momentum decomposed DOS divided by total DOS at Fermi level for FCC Li, Na, K, Rb, and Cs with volume using FP method. The dashed line is the phase border.

all the calculated FSN and dynamic instability features, together with previously theoretical results and experimental measurements for these five alkali metals to provide a full review for the readers. We found two distinct phonon-softening behaviors for Rb at wave vectors 0.3(110) and 0.6(110). However, at the pressure corresponding to the phase transition, the TA phonon frequency at 0.3(110) becomes imaginary but the phonon mode at wave vector of 0.6(110) is still positive and therefore still dynamically stable. Thus, the phonon softening at 0.3(110) is the primary cause for the pressure-induced phase transition.

It is very important to note that the nature of the pressure-induced phonon softening predicted for Rb and Cs[22] is quite different from that for Li,[14,15] Na, and K. For Rb and Cs, the soft phonon was found to occur near the zone center with an incommensurate softening vector of (0.3, 0.3, 0). The slopes of phonon dispersions when $\boldsymbol{q} \rightarrow 0$ are related to the elastic constants of a material.[22] For a fcc solid, when $\boldsymbol{q} \rightarrow 0$ along the (110) direction $\rho u_T^2 = (C_{11} - C_{12})/2$, $\boldsymbol{\rho}$ is the atomic density, $u_T = d\omega_T/dq$, $\omega_T = 2\pi v_T$ (v_T is TA phonon frequency). In the case of fcc Rb, the TA phonons along [110] soften and become imaginary at 17 GPa [Fig. 9(d)]. At this pressure, the tetragonal shear elastic constant $C' = (C_{11} - C_{12})/2$ becomes negative. This observation is similar to that found in Cs[22] earlier. It is significant to point out that the present theoretical results of the similar phonon softening and the FSN behavior shown in Figs. 6 and 7 parallel the experimental observations on the similar phase transition sequence from fcc (Fm-3m) to $C222_1$ in Rb and Cs.

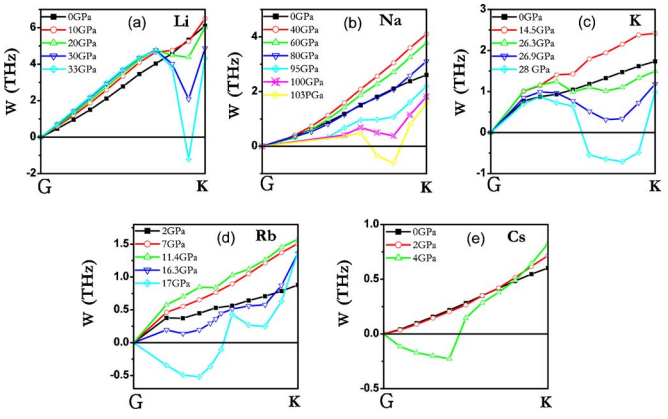

FIG. 9. (Color online) Calculated phonon dispersions of fcc Li (a), Na (b), K (c), Rb (d), and Cs (e) along the Γ-K direction with pressure for TA phonon modes (frequencies below the zero axis denote imaginary values). The phonons become unstable around the K symmetry point at 33 GPa for Li, 103 GPa for Na and 28 GPa for K, and near the zone center at 17 GPa for Rb and at 4 GPa for Cs, respectively.

In contrast, for fcc Li,[14] Na, and K, the TA phonon frequencies along [110] soften and become imaginary frequency at similar incommensurate softening vectors of ~(0.65, 0.65, 0) or (0.6, 0.6, 0) near the K symmetry point with increasing pressure [Figs. 9(a)–9(c)] as listed in Table II. Since the phonon instabilities do not occur near the zone center, consequently there is no weakening of the shear elastic modulus C'. The apparent difference in the pressure-induced phonon softening behavior between heavier alkali (Rb and Cs) and lighter alkali (Li, Na, and K) shed strong light on the reason behind the different high-pressure structures. It is clear that Li, Na, and K take a different route to the pressure-induced post-fcc phases than those of Rb and Cs. Very recently, McMahon *et al.*[10] observed that fcc K transforms to a host-guest composite structure comprising the same 16-atom host structure as Rb-IV and a C-face-centered, rather than a body-centered, tetragonal, guest structure. On the other hand, fcc Li transforms to a rhombohedral cell containing one atom with a space group of R-3m.[9] For fcc Na, Hanfland *et al.*[4] observed a phase transition to a low-symmetry structure at pressures beyond 103 GPa. This structure was suggested to be a body-centered cubic structure with space group of I-43d.[13,38] So far, there is

TABLE II. Calculated phonon softening wave vectors (q) and transition pressures (P_t^P), and FSN wave vectors (k) and transition pressures (P_t^F) for fcc Li, Na, K, Rb, and Cs, respectively. Previous theoretical calculations (Refs. 15 and 22) on phonon softening wave vectors (q) and transition pressures (P_t^P) for Li and Cs, and the experimental measurements (Refs. 4, 5, 9, 11, and 12) on the phase transition pressures for five alkali metals are shown for comparison. The experimentally measured (Refs. 9–12) post-fcc structures for Li, K, Rb, and Cs, and the proposed (Ref. 13) post-fcc phase structures for Na are also listed.

	Experimental observations		Phonon instability		Fermi surface nesting	
	Post-fcc phases	P_t^E (GPa)	Wave vector q $(2\pi/a_0)$	P_t^P (GPa)	Wave vector k $(2\pi/a_0)$	P_t^F (GPa)
Li	R-$3m$[a]	39[a]	(0.7, 0.7, 0) (0.65, 0.65, 0)[b]	33 35[b]	0.71(110)	30
Na	I-$43d$[c]	103[d]	(0.6, 0.6, 0)	103	…	…
K	Host-gust composite structure[g]	19[f]	(0.6, 0.6, 0)[e] (0.6, 0.6, 0)	31[e] 28	0.58 (110)	18
Rb	$C222_1$[h]	13[h]	(0.3, 0.3, 0)	17	0.58(110)	13.2
Cs	$C222_1$[i]	4.2[i]	(0.3, 0.3, 0) (0.3, 0.3, 0)	4.0 5.2[j]	0.58(110)	4

[a]Reference 9.
[b]Reference 15.
[c]Reference 13.
[d]Reference 4.
[e]Reference 16.
[f]Reference 5.
[g]Reference 10.
[h]Reference 11.
[i]Reference 12.
[j]Reference 22.

no detailed experimental report on this structure.

To understand the difference in the phase transition sequence of fcc Li, Na, and K, two important points need to be recognized. It is found that a very similar TA phonon softening behavior occurs upon compression along the Γ-K direction for the three metals as shown in Fig. 9 and listed in Table II. In contrast, the evolution of the FS and the appearance of the FSN behavior for these metals were very different. Specifically, a FSN in the (110) plane along Γ-K direction with a nesting vector of 0.71(110) was observed in Li. No FSN feature that might lead to structural instability was found in Na up to 242 GPa. Finally, in K the FSN feature appears in the (100) plane with an incommensurate nesting vector of 0.58(110).

In the present study, it is found that FSN and soft phonons can coexist at pressure close to the observed structural transitions. In principle, both electronic (FSN) and phonon softening can induce a structural instability, thus resulting in a phase transition. It is nontrivial to distinguish the dominating factor driving the phase transition. Several important aspects of the transition must be considered. Firstly, even though no FS (electronic) instability is predicted for Na, there exists a dynamical (phonon) instability that may induce a phase transition from the fcc to the high-pressure phase. Secondly, although a similar phonon softening was predicted near the K symmetry point in Li and K, very different FSNs were found which result in different high-pressure structures. Thirdly, Rb and Cs possess similar electronic and phonon instabilities and also exhibit a similar phase transition sequence and closely related high-pressure structures. For both metals, the succeeding high-pressure phases have a complex and modulated structure.[11,12]

Among the alkali metals, high-pressure post-fcc structures have only been unambiguously determined for Li, K, Rb, and Cs. With the limited experimental results in combination with the current calculations, we can make the following remarks. Besides for Na, it is also proposed that the TA phonon softening is responsible for the phase transition in fcc Li. A phonon-driven fcc→rhombohedral transformation follows the *normal* sequence of high-pressure transformation. Rhombohedra is a subgroup of hexagonal and therefore the general sequence for increasing dense packing bcc →fcc→hexagonal is followed. Furthermore, a shear instability can easily distort an fcc unit cell into a rhombohedral structure. The situation in Rb and Cs is more complicated. There is obviously a competition between FSN and phonon softening instabilities. If FSN indeed drives the transition, it will be likely analogous to a charge density wave distortion (CDW) resulting in a modulated structure.[20] Both Rb and Cs transform to the $C222_1$ structure but with different stacking of atomic layers along the c axis before reaching more *regular* and simplistic tetragonal $I4_1/amd$ structure at higher pressure. The observed modulation in atomic layers for Rb and Cs within $C222_1$ structure is a strong hint of CDW distortion. It is noteworthy that the post-fcc structures for Li, R-$3m$ and $cI16$ are not modulated.

In conclusion, the FS and phonon lattice dynamics at high pressure fcc alkali metals have been investigated extensively using *ab initio* method within the density functional theory. Fermi surface nesting along Γ-K in the Brillouin zone is identified for Li with a nesting vector of 0.71 (110), K, Rb, and Cs with a nesting vector of 0.58 (110), while no distortion of the free-electron-like FS for Na was found. A TA phonon softening along Γ-K with pressure is predicted for all

fcc alkali metals. Analysis of the calculated results suggested that it is crucial to understand the pressure-induced phase transitions in alkali metals from fcc to lowly coordinated structures by combining the FSN and the phonon softening.

We are thankful for financial support from the China 973 Program under Grant No. 2005CB724400, the NSAF of China under Grant No. 10676011, the National Doctoral Foundation of the China Education Ministry under Grant No. 20050183062, the SRF for ROCS and SEM, the Program for 2005 New Century Excellent Talents in University, and the 2006 Project for Scientific and Technical Development of Jilin Province. J.S.T. wishes to thank NSERC, CFI, and the Canada Research Chair Program for financial support. A large part of the calculations in this work were performed using the QUANTUM-ESPRESSO package.[39]

*Corresponding author. Electronic mail: mym@jlu.edu.cn

[1] E. Wigner and F. Seitz, Phys. Rev. **43**, 804 (1933).
[2] A. Rodriguez-Prieto and A. Bergara, Phys. Rev. B **72**, 125406 (2005).
[3] B. Olinger and W. Shaner, Science **219**, 1071 (1983).
[4] M. Hanfland, I. Loa, and K. Syassen, Phys. Rev. B **65**, 184109 (2002).
[5] K. Takemura and K. Syassen, Phys. Rev. B **28**, 1193 (1983).
[6] K. Takemura and K. Syassen, Solid State Commun. **44**, 1161 (1982).
[7] H. T. Hall, L. Merrill, and J. D. Barnett, Science **146**, 1297 (1964).
[8] J. C. Duthie and D. G. Pettifor, Phys. Rev. Lett. **38**, 564 (1977); H. L. Skriver, Phys. Rev. B **31**, 1909 (1985); A. K. McMahan, *ibid.* **29**, 5982 (1984).
[9] M. Hanfland, K. Syassen, N. E. Christensen, and D. L. Novikov, Nature (London) **408**, 174 (2000).
[10] M. I. McMahon, R. J. Nelmes, U. Schwarz, and K. Syassen, Phys. Rev. B **74**, 140102(R) (2006).
[11] R. J. Nelmes, M. I. McMahon, J. S. Loveday, and S. Rekhi, Phys. Rev. Lett. **88**, 155503 (2002).
[12] M. I. McMahon, R. J. Nelmes, and S. Rekhi, Phys. Rev. Lett. **87**, 255502 (2001).
[13] H. Katzke and P. Tolédano, Phys. Rev. B **71**, 184101 (2005).
[14] D. Kasinathan, J. Kuneš, A. Lazicki, H. Rosner, C. S. Yoo, R. T. Scalettar, and W. E. Pickett, Phys. Rev. Lett. **96**, 047004 (2006).
[15] G. Profeta, C. Franchini, N. N. Lathiotakis, A. Floris, A. Sanna, M. A. L. Marques, M. Lüders, S. Massidda, E. K. U. Gross, and A. Continenza, Phys. Rev. Lett. **96**, 047003 (2006).
[16] A. Sanna, C. Franchini, A. Floris, G. Profeta, N. N. Lathiotakis, M. Lüders, M. A. L. Marques, E. K. U. Gross, A. Continenza, and S. Massidda, Phys. Rev. B **73**, 144512 (2006).
[17] J. S. Tse, Y. Ma, and H. M. Tutuncu, J. Phys. Condens. Matter **17**, S911 (2005).
[18] L. Shi and D. A. Papaconstantopoulos, Phys. Rev. B **73**, 184516 (2006).
[19] L. Shi and D. A. Papaconstantopoulos, and M. J. Mehl, Solid State Commun. **127**, 13 (2003).
[20] E. Canadell and M. H. Whangbo, Chem. Rev. (Washington, D.C.) **91**, 965 (1991).
[21] S. Baroni, S. de Gironcoli, A. Corso, and P. Gianozzi, Rev. Mod. Phys. **73**, 515 (2001).
[22] J. Xie, S. P. Chen, J. S. Tse, D. D. Klug, Z. Li, K. Uehara, and L. G. Wang, Phys. Rev. B **62**, 3624 (2000).
[23] A. Rodriguez-Prieto and A. Bergara, *20th AIRAPT*, Karlsruhe, Germany, 2005.
[24] S. Baroni, P. Giannozzi, and A. Testa, Phys. Rev. Lett. **58**, 1861 (1987).
[25] W. Kohn and L. J. Sham, Phys. Rev. **140**, A1133 (1965).
[26] N. Troullier and J. L. Martins, Phys. Rev. B **43**, 1993 (1991).
[27] P. Blaha, K. Schwarz, G. K. H. Madsen, D. Kvasnicka, J. Luitz, WIEN2K, An Augmented-Plane-Wave+Local Orbitals Program for Calculating Crystal Properties, Karlheinz Schwarz, Techn. Wien, Austria, 2001, ISBN 2-9501031-1-2.
[28] P. Hohenberg and W. Kohn, Phys. Rev. **136**, B864 (1964).
[29] J. P. Perdew and K. Burke, Int. J. Quantum Chem. **57**, 309 (1996); J. P. Perdew, K. Burke, and M. Ernzerhof, Phys. Rev. Lett. **77**, 3865 (1996).
[30] F. Birch, Phys. Rev. **71**, 809 (1947).
[31] M. M. Dacorogna and M. L. Cohen, Phys. Rev. B **34**, 4996 (1986).
[32] M. Sigalas, N. C. Bacalis, D. A. Papaconstantopoulos, M. J. Mehl, and A. C. Switendick, Phys. Rev. B **42**, 11637 (1990).
[33] M. S. Anderson and C. A. Swenson, Phys. Rev. B **31**, 668 (1985).
[34] M. Winzenick, V. Vijayakumar, and W. B. Holzapfel, Phys. Rev. B **50**, 12381 (1994).
[35] K. Takemura, S. Minomura, and O. Shimomura, Phys. Rev. Lett. **49**, 1772 (1982).
[36] K. Iyakutti and C. N. Louis, Phys. Rev. B **70**, 132504 (2004).
[37] J. B. Neaton and N. W. Ashcroft, Phys. Rev. Lett. **86**, 2830 (2001).
[38] N. E. Christensen and D. L. Novikov, Solid State Commun. **119**, 477 (2001).
[39] S. Baroni, A. Dal Corso, S. de Gironcoli, P. Giannozzi, C. Cavazzoni, G. Ballabio, S. Scandolo, G. Chiarotti, P. Focher, A. Pasquarello, K. Laasonen, A. Trave, R. Car, N. Marzari, and A. Kokalj, http://www.pwscf.org.